



ELSEVIER

Physics of the Earth and Planetary Interiors 131 (2002) 225–235

PHYSICS
OF THE EARTH
AND PLANETARY
INTERIORS

www.elsevier.com/locate/pepi

The implications of non-suppressed geomagnetic secular variation during the Permo-Carboniferous Reversed Superchron

Pauline P. Kruiver^a, Cor G. Langereis^{a,*}, Mark J. Dekkers^a,
Gareth R. Davies^b, Richard J. Smeets^b

^a Paleomagnetic Laboratory Fort Hoofddijk, Utrecht University, Budapestlaan 17, 3584 CD, Utrecht, The Netherlands

^b Faculty of Earth Sciences, Vrije University, De Boelelaan 1085, 1081 HV, Amsterdam, The Netherlands

Received 18 July 2001; accepted 30 April 2002

Abstract

We have investigated variations in the natural remanent magnetisation (NRM) in red beds which were deposited during the Permo-Carboniferous Reversed Superchron (PCRS) near the paleo-equator. These red beds are reliable recorders of the geomagnetic field, because the NRM is carried by detrital hematite. We analysed the angular standard deviation (ASD) and spectral content of the directional records to quantify the amount of paleosecular variation (PSV) during the time of deposition. The ASD of a high-resolution directional record of the Dôme de Barrot which spans approximately 27 kyr is 10° . This is comparable to recent (0–5 Ma) low-latitude lavas from the PSVRL database (McElhinny and McFadden, 1997) and to recent lake sediments from the SECVR database (McElhinny and Lock, 1996). The frequency spectra of declination and inclination are also similar to those from the recent lake sediments: spectral power significant at the 95% level is concentrated in periods of ~1–5 kyr, higher frequencies are not significant. From the ASD and spectral analyses, it appears that the amount of PSV during—at least part of—the PCRS was comparable to that of recent times. Several heuristic and numerical geodynamo models are discussed in the context of Superchrons and PSV. There is a discrepancy between the amount of SV shown by our data and that suggested by numerical models which use lateral heat flux variations at the core–mantle boundary (CMB). However, computational limitations still force some model parameters to have values that are unrealistic for the Earth. For the phenomenological geodynamos, ‘low-energy state’ models which suggest that PSV is suppressed during a Superchron are not supported by the Dôme de Barrot data. Rather, a ‘high-energy state’ of the geodynamo, in which outer-core convection is vigorous, is favoured as a prerequisite for a Superchron to occur.

© 2002 Elsevier Science B.V. All rights reserved.

Keywords: Superchron; Secular variation; Geodynamo models; Angular standard deviation; Spectral analysis

1. Introduction

Prominent features of the geomagnetic field are governed by processes which operate on vastly different time scales. Variations in the directions of the geo-

magnetic field with an internal source range from the 1 year time scale of magnetic ‘jerks’ (e.g. Alexandrescu et al., 1997), via variations on time scales of 10^2 to 10^4 years for secular variation (SV), excursions and reversals, to the 10^5 to 10^6 years time scale of magnetic polarity chrons (e.g. McFadden and Merrill, 1997). Superchrons, i.e. long periods without reversals, occur on even longer time scales of 10^7 years. Examples are the Cretaceous Normal Superchron

* Corresponding author. Tel.: +31-30-253-1672;

fax: +31-30-253-1677.

E-mail address: langer@geo.uu.nl (C.G. Langereis).

(CNS) from 120 to 83 Ma (Gradstein et al., 1995) and the Permo-Carboniferous Reversed Superchron (PCRS) from 311 to 262 Ma (Opdyke, 1995).

The characteristics of the geomagnetic field during the last 5 Myr have been extensively investigated. McElhinny et al. (1996), for example, showed that there is no statistically significant difference between the time-averaged normal and reversed polarity states. Anomalous behaviour of the time-averaged geomagnetic field coincides with seismic velocity heterogeneities in the lower mantle and at the core–mantle boundary (CMB) (Johnson and Constable, 1997). The character of paleosecular variation (PSV), for instance the latitude dependence of angular standard deviation (ASD) of the virtual geomagnetic poles (VGPs), is described by McElhinny and McFadden (1997). Knowledge of secular variation behaviour is important, because it puts constraints on geodynamo models. SV has time scales typical of outer-core convection processes (overturn time ~ 500 years; Gubbins, 1999) and the inner-core diffusion time (~ 3000 years; Hollerbach and Jones, 1993). In recent years, several models addressing the geomagnetic field have been published (Courillot and Besse, 1987; Larson and Olson, 1991; McFadden et al., 1991; Glatzmaier and Roberts, 1995; McFadden and Merrill, 1995; Kuang and Bloxham, 1997). Some of these models predict PSV to be suppressed during a Superchron, while others expect it to be comparable to present-day SV.

An excellent opportunity to test the validity of geodynamo model predictions which discuss the amount of PSV is provided by the Permian red beds of Dôme de Barrot, south-eastern France. These red beds were deposited during the PCRS near the paleo-equator. Kruiver et al. (2000) showed that the patterns of the natural remanent magnetisation (NRM) in these sediments closely resemble those of present-day secular variation. They verified that the remanence is a depositional remanent magnetisation (DRM) of purely detrital origin, carried by hematite. No signs of diagenetic influences on the NRM were detected. The directional results can, therefore, be interpreted as variations in the geomagnetic field. In this contribution, we investigate PSV by analysis of the ASD with a variable cut-off angle (Vandamme, 1994). The ASD values are compared to those derived from databases of lavas (0–5 Ma) (McElhinny and McFadden, 1997) and recent lake sediments (McElhinny and Lock, 1996). Additionally,

we perform spectral analysis on our directional records and compare the results with spectra from the lake sediment database. Our analyses suggest that PSV was not suppressed during the PCRS. Finally, we discuss the geomagnetic implications of non-suppressed secular variation during a Superchron for geodynamo models.

2. The age of Dôme de Barrot

The polarity of the sampled stratigraphic series in Dôme de Barrot is reversed (van den Ende, 1977; Kruiver et al., 2000). We need to ascertain that the Dôme de Barrot red beds were indeed deposited during the PCRS and not during one of the reversed Permian polarity chrons post-dating the PCRS. For this purpose, we took oriented hand samples at 10 sites along the entire eastern side of the Dôme de Barrot, so that as much stratigraphic distance as possible is covered. Standard paleomagnetic cores were drilled in the laboratory. Stepwise thermal demagnetisation isolated the characteristic NRM directions, yielding reversed polarities for all samples. Assuming a constant sedimentation rate of ~ 12 cm kyr⁻¹ (Kruiver et al., 2000), and a total thickness of the Dôme de Barrot red bed sequence of ~ 1000 m (van den Ende, 1977), the covered time span of reversed polarity is estimated to be at least ~ 8 Myr. This confirms that the sequence was indeed deposited during the PCRS, since younger Permian polarity chrons have far shorter durations, of ca. 1 Myr or less (Opdyke, 1995).

The age of the section can be constrained by considering palynological data from the Léouvé Formation which forms the top of the Dôme de Barrot sequence. Visscher et al. (1974) assigned a Late Permian age to the pollen. Recently, Permian chronostratigraphy has been considerably revised (Yugan et al., 1997; Wardlaw, 2000). Visscher now assigns a Guadalupian age to the pollen (personal communication). Considering the time span covered by the Dôme de Barrot sequence, it must be placed within the PCRS. Therefore, a Wordian or Roadian age (265–269 Ma; Wardlaw, 2000) is probable for the Léouvé Formation. The end of the PCRS is dated at 262–264 Ma (Opdyke, 1995; Yugan et al., 1997). Therefore, the Dôme de Barrot red beds were deposited during a period in the youngest part of the PCRS.

In an attempt to provide absolute ages we sampled two tuff layers at the eastern side of the Dôme de Barrot. Both tuff layers contained zircons, apatites and titanites. U–Pb ages were determined by thermal ionisation mass spectrometry at the Free University of Amsterdam and at ETH-Zentrum, Zürich. Several zircon, apatite and titanite fractions were analysed on the basis of size, shape and colour. Each mineral contained populations of mixed provenance such that U–Pb and Pb–Pb ages ranged from 410 Ma to more than 1.8 Ga. It was not possible to obtain concordant U–Pb ages. Unfortunately, we must conclude that the tuff layers contain a significant population of reworked sedimentary material which mitigates against a precise absolute age determination.

3. Comparison of the secular variation recorded in Dôme de Barrot red beds with paleomagnetic secular variation databases

3.1. Analysis of ASD

There are several ways to characterise PSV. One method is to draw random samples from a period which is long enough to average SV and calculate the ASD. For the CNS, [McFadden and Merrill \(1995\)](#) determined the ASD from lavas, measured by the global integral of the local SV over all latitudes averaged over the temporal interval of 80–110 Ma. They concluded that PSV was low during the CNS. The dynamo would be in a ‘steady’ state, in contrast to the ‘oscillatory’ state with frequent reversals of the past tens of millions of years. In this study, we take a different approach. We investigate the high-resolution patterns of PSV of continuous sedimentary sections by analysing ASD values with the method of [Vandamme \(1994\)](#). In this method, the mean poles and ASD values (with 95% confidence limits; [Cox, 1969](#)) are determined with a variable cut-off angle defined by the data. In this way, excursions data which would bias the ASD are rejected from the data set. The optimal cut-off angle is determined for each record by iteration. The resulting ASD can then be compared to, for instance, the ASD at a certain latitude during the last 5 Myr ([McElhinny and McFadden, 1997](#)) or during any other period ([McFadden and McElhinny, 1984](#)).

The ASD values from the Dôme de Barrot red beds are compared to ASD values from 18 recent lake sediment sequences for North America and Europe from the ‘Secular Variation’ (SECVR) database ([McElhinny and Lock, 1996](#)). All inclinations and declinations were transformed to VGPs before calculating the ASD values. The results are shown in [Table 1](#) and [Fig. 1](#), together with the Dôme de Barrot ASD results. ASD values range from 5.7 to 19.5°. For the lake sediments, the cut-off angle with the Vandamme method ranges 15–40°, which is lower than the fixed cut-off angle typically taken at 40°.

The ASD values of low-latitude lavas from the ‘Paleosecular Variation from Lavas 0–5 Ma’ (PSVRL) database ([McElhinny and McFadden, 1997](#)) were also calculated for comparison with our low-latitude sediments ([Fig. 1](#)). In general, the ASD of recent lake sediments is lower than that of lavas. In sediments, there is always a certain degree of smoothing of the geomagnetic signal, because of the DRM acquisition mechanism and specimen size. Thus, the ASD recorded by sediments is always a minimum estimate of true SV. The degree of smoothing depends on the sedimentation rate, grain size, lock-in window and burrowing. Lowering the sedimentation rate increasingly smoothes the geomagnetic signal. For series GC (standard size of 10.5 cm³ and a sedimentation rate of 11.8 cm kyr⁻¹; [Kruiver et al., 2000](#)), the geomagnetic signal is averaged over approximately 200 years. In series H (3.5 cm³ samples) approximately 100 years are averaged. The low ASD values of some lake sediments ([Fig. 1](#) and [Table 1](#)) might be explained by smoothing. There is, however, no significant relationship between sedimentation rate and mean ASD ([Fig. 2a](#)) for the lake records. It should be noted that all records have sedimentation rates in excess of 10 cm kyr⁻¹. A relationship between ASD and sedimentation rate might exist for lower sedimentation rates. On the other hand, record length can be important: the mean ASD and record length are correlated ($r = 0.51$), significant at a 95% confidence level ([Fig. 2b](#)). For short records, SV is not averaged which results in low values of ASD. In longer records, the recorded SV represents a more complete picture of the full SV which causes an increase in ASD. For even longer records, the ASD should be independent of record length, because the complete range of SV is recorded. This flattening of the curve is not observed here. The ASD of the two

Table 1
Angular standard deviations for databases and Dôme de Barrot

	(Paleo)	(Paleo)	Record		Average sedimentation rate (cm kyr ⁻¹)	#Poles before selection ^a	#Poles after selection ^a	#Optimal cut-off	longitude mean pole	Latitude mean pole	<i>k</i>	a95	ASD _{low}	ASD _{mean}	ASD _{high}	Reference
	latitude site	longitude site	From (ka)	To (ka)												
Lake sediments North America																
Ch'jee's Bluff	67.6°N	138.9°W	No age information			253	210	31.7	57.5	80.0	30.3	1.8	13.9	14.8	15.9	1
Kylen Lake	47°N	91.8°W	No age information			331	325	26.6	211.8	83.9	46.1	1.2	11.3	12.0	12.7	2
Lake St. Croix	45°N	92.8°W	No age information			290	274	28.3	45.0	87.8	39.5	1.4	12.2	12.9	13.8	2
Mystery Cave Stalagmite	50.5°N	126.7°W	No age information			38	38	30.1	353.4	88.4	34.1	4.0	12.0	13.9	16.5	3
Old Crow River 1	67.8°N	139.8°W	No age information			254	249	34.2	44.8	77.3	25.3	1.8	15.3	16.2	17.3	4
Old Crow River 2	67.8°N	139.9°W	No age information			407	372	40.0	56.5	79.3	17.6	1.8	18.5	19.5	20.6	5
Anderson Pond	36°N	85.5°W	12.5	19.0	37	278	276	26.5	93.6	87.8	46.3	1.3	11.3	11.9	12.7	6
Bessette Creek	50.1°N	118.9°W	19.5	31.0	151	209	205	22.7	12.7	85.1	68.4	1.2	9.2	9.8	10.5	7
Fish Lake	42.5°N	118.6°W	0.0	10.0	79	268	268	22.8	21.0	85.5	67.8	1.1	9.3	9.9	10.5	8
Lake Waiau	19.8°N	155.5°W	0.0	12.7	40	205	204	17.6	340.7	83.0	134.3	0.9	6.6	7.0	7.5	9
Mara Lake	50.8°N	119°W	0.0	4.7	134	231	231	19.6	58.3	83.8	100.0	0.9	7.6	8.1	8.7	10
Mono Lake	38°N	119°W	12.0	35.0	38	404	385	32.3	94.8	86.0	28.7	1.4	14.4	15.2	16.0	11
Lake sediments Europe																
Loch Lomond	56°N	5°W	0.0	6.0	47	169	169	21.4	105.7	89.0	79.5	1.2	8.5	9.1	9.9	12
Llyn Geirionydd	53°N	3°W	0.0	6.2	46	176	176	15.2	280.5	89.0	203.9	0.7	5.3	5.7	6.1	13, 14
Lake Windermere	54.3°N	3°W	1.5	10.0	28	216	216	17.2	106.2	88.2	143.3	0.8	6.4	6.8	7.3	13, 14
Lake Aslikul	54.4°N	54.1°E	0.5	3.7	70	436	434	19.6	317.8	83.1	100.4	0.7	7.7	8.1	8.5	15
Lake Baikal (Asia)	52.2°N	106.5°E	0.5	12.0	13	76	76	29.0	120.7	83.1	37.1	2.7	12.0	13.3	15.0	16
Lac du Bouchet	44.9°N	3.8°E	12.5	24.5	31	1821	1802	31.2	143.7	89.1	31.4	0.6	13.9	14.5	15.2	17
Dôme de Barrot																
Series GC	8°N		Duration ~26.8 kyr		11.8	90	87	23.4	321.9	-46.0	63.3	1.9	9.2	10.2	11.4	18
Series H	8°N		Duration ~3.2 kyr		11.8	49	49	18.7	315.1	-45.4	114.6	1.9	6.7	7.6	8.8	18
Series ENR	8°N					134	134	18.0	309.7	-45.2	125.3	1.1	6.7	7.3	7.9	19
Series ENE	8°N					88	88	17.2	323.0	-47.8	143.0	1.3	6.1	6.8	7.6	19

Mean poles and ASD values determined using Vandamme (1994) for lake sediments from the SEVCR database and the Dôme de Barrot red beds. Site (paleo)latitudes and longitudes are taken from the SEVCR database. When a time–depth relationship was available, the time interval used for the ASD analysis and the spectral analysis is indicated; *k* is the precision parameter; a95 the semi-angle of the cone of 95% confidence for the mean poles. ASD_{mean}, ASD_{low} and ASD_{high} are mean, lower and upper limit values for angular standard deviation on a 95% confidence level (Cox, 1969). The references are: (1) Evans and Wang (1994); (2) Lund and Banerjee (1985a); (3) Lean et al. (1995); (4) Hedlin and Evans (1987); (5) Gillen and Evans (1989); (6) Lund and Banerjee (1985b); (7) Turner et al. (1982); (8) Verosub et al. (1986); (9) Peng and King (1992); (10) Turner (1987); (11) Lund et al. (1988); (12) Turner and Thompson (1979); (13) Turner and Thompson (1982); (14) Turner and Thompson (1981); (15) Nurgaliev et al. (1996); (16) Peck et al. (1996); (17) Thouveny et al. (1990); (18) Kruiver et al. (2000); (19) van den Ende (1977).

^a Poles before/after selection: number of poles before and after applying the Vandamme (1994) method, which determines the optimal cut-off angle.

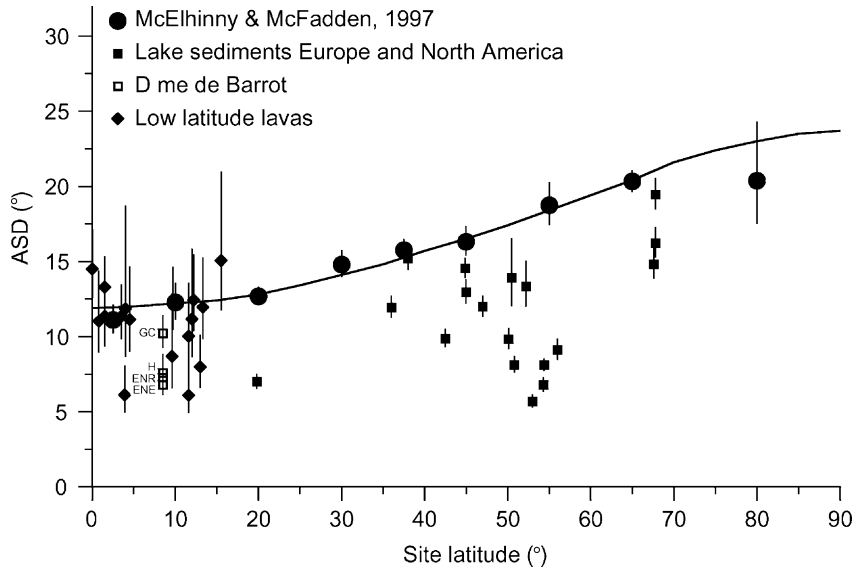


Fig. 1. Latitude dependence of ASD is expressed by the solid black line and latitude band averages (circles) from [McElhinny and McFadden \(1997\)](#). Diamonds represent ASD values for low-latitude lavas (0–5 Ma) from the PSVRL database ([McElhinny and McFadden, 1997](#)). Filled squares represent ASD values for recent lake sediments from North America and Europe from the SECVR database ([McElhinny and Lock, 1996](#)) (Table 1); open squares for the Dôme de Barrot red beds GC and H (this study) and series ENR and ENE ([van den Ende, 1977](#)) (Table 1). Error bars represent 95% confidence limits ([Cox, 1969](#)).

longest records of ca. 25 kyr, however, is not larger than that of most of the records of ca. 12–15 kyr length. So, based on this admittedly low number of records, it is reasonable to consider a record length of 20–25 kyr to represent the full spectrum of secular variation.

For the Permian red beds of the Dôme de Barrot (paleolatitude of ~8°N) the ASD of series GC is 10.2°, agreeing reasonably well with that of low-latitude

lavas. Typically, the ASD values derived from lake sediment records are distinctly smaller than those derived from lava records. The difference between the Dôme de Barrot red beds (especially GC) and the lavas is rather small. Therefore, from the analysis of ASD values we conclude that PSV was not notably suppressed during deposition of these red beds.

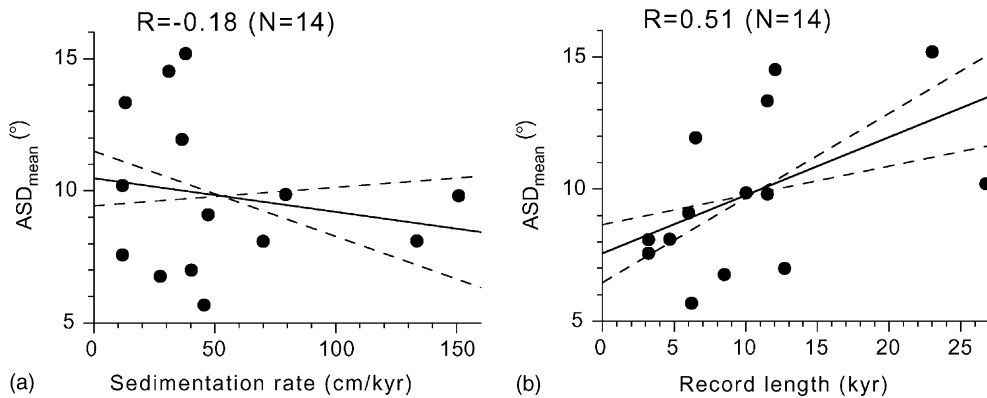


Fig. 2. (a) Mean ASD vs. sedimentation rate; and (b) mean ASD vs. record length for series GC and H and the lake sediment records (Table 1). Dashed lines represent confidence limits for the solid regression line.

The ASD of series H is much lower than of GC. Series H overlaps with series GC, but is too short (~ 3 kyr for H compared to ~ 27 kyr for GC) to contain the full spectrum of secular variation, and is therefore, biased towards lower ASD values. The ASD values of van den Ende's (1977) series ENE and ENR (sampled at approximately the same locality as GC and H) are also relatively low, but van den Ende (1977) based his ASD values on averaged declination and inclination per approximate stratigraphic level, which introduces additional smoothing thereby reducing the ASD.

3.2. Spectral content of lake records and SV

Sedimentary sequences contain continuous records of the geomagnetic field, provided that hiatuses are absent. Given a reliable time–depth relationship for a directional record, spectral analysis has been used as another tool to analyse PSV (Barton, 1982). Spectral analysis has the advantage that it analyses changes in the PSV record rather than absolute values. A cautionary note should be added here: spectral analysis considers numerical values and not vectors. Therefore, the full NRM vector was split into declination and inclination that are given unit length. Trial runs showed that the outcome of this procedure was equivalent to splitting the vector into Cartesian co-ordinates. The normalisation, however, may introduce biasing effects into the spectral analysis and, therefore, we adopted a conservative interpretation cautioning for overinterpretation. We analysed the records of declination and inclination for 11 lake sediment records from North America, Europe and Asia for which an age model was available (McElhinny and Lock, 1996), of which some are shown in Fig. 3. The same parts of the records as used for the ASD analysis were processed (see Table 1).

We used the CLEAN algorithm of Roberts et al. (1987) for the spectral analyses of the directional data from the SECVR database, because it can handle non-equidistant data series without interpolation of data. In the CLEAN procedure, a 'dirty' spectrum is first calculated and then 'cleaned' by iteration. This CLEANing is accomplished by compensating for the largest peak in the spectrum with a given gain. In this way, sidelobes are removed and clean spectral components are retained. After the last iteration, the CLEAN spectrum is constructed from the accumulated clean

spectral components and the residual spectrum. To provide a confidence level for CLEAN spectra, Heslop and Dekkers (2002) performed Monte Carlo simulations. The variability in the measured input spectrum is evaluated by calculating it a 1000 times with the addition of specified amounts of white noise or red noise to be selected by the user. Alternatively, the measured input data can be stripped down to a percentage also selected by the user. The random stripping is also performed 1000 times. The Monte Carlo spectrum shows a band of possible frequency powers and a 95% confidence level. Regardless of the method chosen, essentially the same confidence levels were produced. Spectral peaks above this confidence level are regarded as significant. Simulations of Heslop and Dekkers (2002) on an input record consisting of a 500 kyr segment of the Laskar (1990) insolation curve randomly stripped to 80% of the original record and with 100% white or red noise added to it, showed that further addition of up to 50% of white noise to this input record did not seriously affect the resulting Monte Carlo CLEAN spectra. For the present study we selected a level of white noise of 20%.

The frequency spectrum of a directional record is often calculated by first determining the spectra for declination and for inclination separately. Then, the total spectrum for each record can be obtained by adding the two spectra at each frequency (Barton, 1982). The Monte Carlo CLEAN procedure, however, results in an error band and a 95% confidence level, which is generally not identical for declination and inclination. Therefore, we display the spectra of both declination and inclination separately, and do not add them together. The spectra of declination and inclination for seven lake sediment records and for series GC from Dôme de Barrot are shown in Fig. 3. Differences in sedimentary environment of the various lakes inevitably must result in different filtering characteristics of the NRM, and explain at least part of the observed variability. The variability may additionally be explained by the differences of the lake records both in time and space (cf. Table 1). Indeed, historical records show that secular variation may considerably differ spatially and temporally over the globe. In records of sufficient length, however, we expect the longer-term SV characteristics to become comparable. The nature of SV as well as the intricacies of the recording process, however, require a conservative

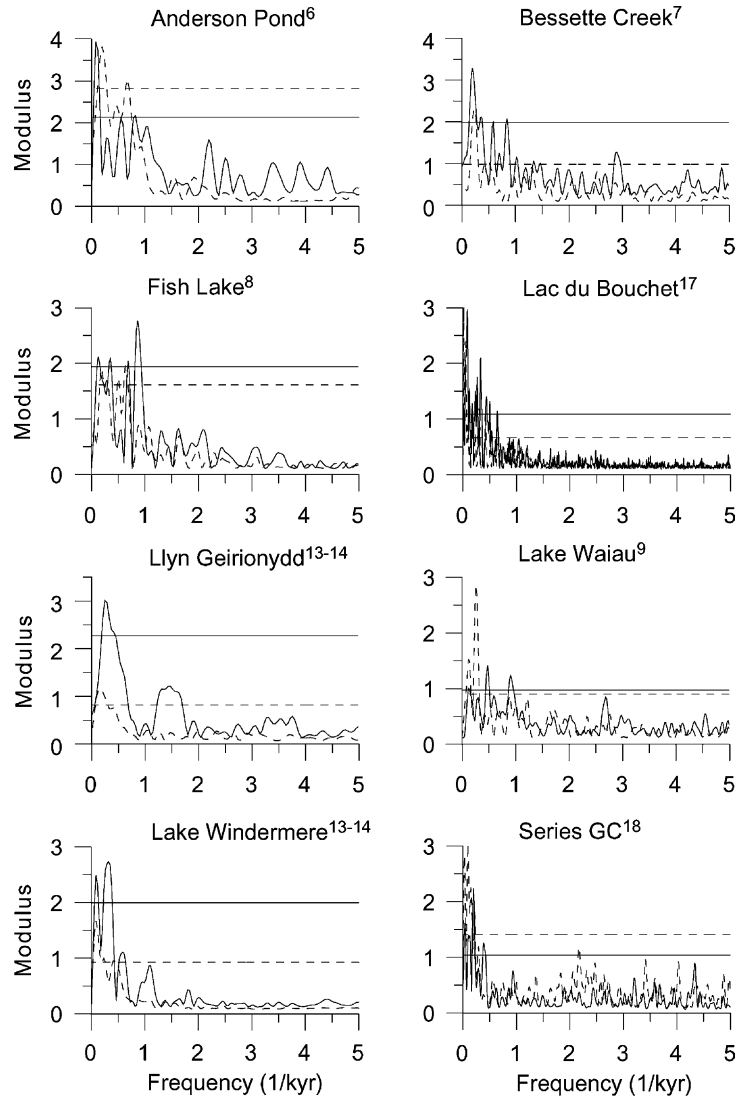


Fig. 3. Monte Carlo CLEAN frequency spectra of declination (solid line) and inclination (dashed line) for several lake sediment records of the SECVR database (McElhinny and Lock, 1996) and series GC. The 95% confidence band of spectral power is so tight that the spectra appear as a thick line rather than a band. Solid (dashed line) horizontal lines indicates 95% confidence levels for declination (inclination). Monte Carlo CLEAN parameters were: level of added white noise = 20%, level of confidence = 95%, gain = 0.1, $dT = 50$, 1000 iterations. Numbers indicated as superscripts in the lake name correspond to references in Table 1.

approach and we consider only the most robust features.

The spectral analysis shows that the variability in spectral content between the lake records is considerable. It is evident, however, that all variability with periods less than 1000 years is not significant. This would imply that the short duration components in

secular variation have a random character which is concurrent with SV observed in historical records. The overall conformity between the records is that the significant spectral peaks have periods ranging ~ 1000 – 2000 to 5000 years; longer periods should be regarded with some caution, given the length of some of the lake records. In the few spectra which

span the same time interval, there appears to be no typical or dominant period. This would plead for a random character of any longer SV periods and/or quite different sedimentary recording mechanisms.

For the determination of the spectral content of series GC, the stratigraphic distance is converted to time, using an average sedimentation rate of 11.8 cm kyr^{-1} (Kruiver et al., 2000). Its duration is approximately 27 kyr, thus, representing one of the longer records. The variability of the GC spectrum is comparable to that of the lake spectra. The best-quality records of Lac du Bouchet and of Lake Windermere, have closest resemblance to the GC record, but only in the sense that the significant periods are longer than ca. 1500 years. Series H consists of only 49 data points, which precludes the construction of sensible spectra.

4. Implications for geodynamo theory

4.1. Geodynamo models

From the previous section it emerges that the Dôme de Barrot red beds indicate that PSV was not suppressed during—at least part of—the PCRS. Here, we discuss some of these models in the context of Superchrons and SV. There are many geodynamo models, ranging from phenomenological models to numerical computer simulations. Most geodynamo models assume that D'' represents a thermal boundary layer. Deep-mantle plumes can erupt from this layer (e.g. Loper and McCartney, 1986; Sheridan, 1986; Courtillot and Besse, 1987; Larson and Olson, 1991) or cold mantle material descends through the mantle and comes to rest at the D'' layer (e.g. Eide and Torsvik, 1996; Gallet and Hulot, 1997). These cold or hot anomalies can change the thermal conditions, and the lateral pattern of heat flux at the CMB. In the numerical geodynamo models the properties of the D'' layer and of the inner–outer-core boundary constrain the boundary conditions.

In the phenomenological models, there are two contradictory concepts for the explanation of the existence of Superchrons: some models require a ‘low-energy state’ of the geodynamo as a prerequisite for a Superchron (Loper and McCartney, 1986; Sheridan, 1986; Courtillot and Besse, 1987; McFadden and Merrill, 1995). In these models, it is assumed that each rever-

sal is the outcome of an instability in the outer core. Therefore, outer-core convection would be smooth and without instabilities during a Superchron. Others argue that a Superchron represents a ‘high-energy state’ of the geodynamo in which outer-core convection is more vigorous (Olson and Hagee, 1990; Larson and Olson, 1991; Greff-Lefftz and Legros, 1999).

Fluid flow in the outermost core is linked to SV (Blokhman and Jackson, 1991). SV is, thus, taken as a measure of the vigour of outer-core convection. In the case of models which advocate a ‘low-energy’ geodynamo during a Superchron, SV would be suppressed. On the other hand, for the ‘high-energy’ geodynamo during a Superchron, SV would be ‘normal’ or even enhanced compared to the present-day situation. However, paleomagnetic observations have not been able to unequivocally discard either the ‘high-’ or ‘low-energy state’ models. The statistical analysis of the surface integral of ASD of lavas indicates that SV was reduced during the CNS (McFadden and Merrill, 1995). Also, Rochette et al. (1997) found low ASD values ($4\text{--}8^\circ$) for Permian equatorial lavas from the Esterel, whereas recent (0–3 Ma) equatorial lavas from the Galapagos showed ASD values of $10\text{--}13^\circ$. They concede, however, that the low ASD value for the Permian lavas might have been caused by remagnetisation of the lavas. In addition, the actual number of ignimbritic flows might be lower than considered in the Rochette et al. (1997) study (Zijderveld, personal communication). The relatively high ASD values, general directional characteristics and the spectral content of NRM directions of the Dôme de Barrot red beds, however, suggest that SV was not suppressed during—at least part of—the PCRS.

Lateral variations of heat flux at the CMB are considered to be more important than the total heat flux (Gubbins, 1987). Loper (1992) estimated that the natural time scale of variations in the total heat flux from the core is approximately 10^9 years, which is far longer than the time scales of long-term variations in the reversal frequency of the geomagnetic field. This would imply that the total heat flux from the core is not significantly affected by lower mantle processes and, hence, that other processes must influence the reversal frequency.

Glatzmaier et al. (1999) analysed the effect of varying radial heat flow across the CMB on dynamo action with a magneto-hydrodynamical numerical model.

The most Earth-like dynamo resulted from uniform heat flow conditions. The heat flow pattern derived from tomographic studies of the lower mantle shows magnetic field behaviour which does not agree with paleomagnetic observations. Both the tomographic and homogeneous heat flux models are not representative for Superchrons. Glatzmaier et al. (1999) suggested that the condition for a Superchron is satisfied when the lateral pattern of diffusive heat flux from the core to the mantle matches the natural time-averaged pattern of convective heat flux deep within the fluid core. This occurs in their simulations when the CMB heat flux is axisymmetric and symmetric around the equator, thus, with maxima in the polar regions. This only non-reversing geodynamo simulation displays very little SV, with a high and variable dipole moment.

On the other hand, it is conceivable that when the pattern of lateral diffusive heat across the CMB is in phase with the convective heat flux pattern in the outer core, that the geodynamo would be ‘boosted’ into a ‘high-energy state’ (and, thus, high dipole moment). This could be accompanied by strong outer-core convection, resulting in large SV. This would be in agreement with what we observe, but contrary to the calculations of Glatzmaier et al. (1999). A CMB heat flux pattern that explains both strong dipole moment and large SV might exist, for instance with a combination of high polar heat flux and lower but non-zero heat flux at the equator. Glatzmaier et al. (1999), however, caution that the simulations are too short to allow firm conclusions. Moreover, a much more realistic viscosity (smaller Ekman number) and smaller time steps are needed to better tie the model to conditions in the Earth.

4.2. CNS versus PCRS

The phenomenological models are all formulated for the CNS. It must be noted, however, that the global regimes preceding and during the CNS and the PCRS were fundamentally different. The PCRS corresponds to a period of continental assembly, while the CNS post-dates a prolonged period of supercontinental mantle insulation followed by continental break-up (Eide and Torsvik, 1996). Essentially, this means that models designed for the CNS do not necessarily apply to the PCRS and vice versa. In the extreme case, the state of the geodynamo might be fundamentally dif-

ferent for both Superchrons. Greff-Lefftz and Legros (1999) showed that the rotational eigenfrequencies of the liquid outer-core and solar gravitational tidal waves were in resonance at 3.8 ± 0.2 , 3.0 ± 0.2 , 1.8 ± 0.2 Ga and 300 ± 100 Ma. From their analysis, it thus appears that resonance occurred during the PCRS, but not during the CNS. Greff-Lefftz and Legros (1999) suggest that during times of resonance the inner-core growth stopped, leading to a new momentum equilibrium for the geodynamo and enhanced outer-core convection.

It has to be noted that the amount and character of SV would be similar during an entire Superchron. Since the Dôme de Barrot red beds were deposited near the end of the PCRS, prevailing conditions might have been different from those at the start or in the middle of the Superchron. If SV were suppressed during the CNS, but not suppressed during the PCRS, this would suggest that the geodynamo was fundamentally different during both Superchrons. However, if Superchrons represent the same geodynamo regime, our findings do not support the ‘low-energy’ geodynamo models and are in favour of the ‘high-energy’ geodynamo models. Lateral variations in heat flux at the CMB, however, might be more important than the total global heat flux.

Acknowledgements

We thank Charlotte Egmond for analysing part of the databases, Didier Vandamme for providing us with the variable cut-off angle computer program and Dave Heslop for his help with the spectral analysis. Urs Schaltegger is sincerely thanked for performing the U–Pb zircon analyses. This work was conducted under the programme of the Vening Meinesz Research School of Geodynamics (VMSG) and funded by The Netherlands Organisation for Scientific Research (NWO/ALW).

References

- Alexandrescu, M., Courtillot, V., Le Mouél, J.-L., 1997. High-resolution secular variation of the geomagnetic field in western Europe over the last 4 centuries: comparison and integration of historical data from Paris and London. *J. Geophys. Res.* 102, 20245–20258.

- Barton, C.E., 1982. Spectral analysis of palaeomagnetic time series and the geomagnetic spectrum. *Philos. Trans. R. Soc. Lond. Ser. A* 306, 203–209.
- Bloxham, J., Jackson, A., 1991. Fluid flow near the surface of Earth's outer core. *Rev. Geophys.* 29, 97–120.
- Courtillot, V., Besse, J., 1987. Magnetic field reversals, polar wander, and core–mantle coupling. *Science* 237, 1140–1147.
- Cox, A., 1969. Confidence limits for the precision parameter κ . *Geophys. J. R. Astron. Soc.* 18, 545–549.
- Eide, E.A., Torsvik, T.H., 1996. Paleozoic supercontinental assembly, mantle flushing, and genesis of the Kiaman Superchron. *Earth Planet. Sci. Lett.* 144, 389–402.
- Evans, M.E., Wang, Y., 1994. Palaeomagnetic results from Ch'ijee's Bluff, Porcupine River, Yukon Territory. *Quatern. Inter.* 22, 215–219.
- Gallet, Y., Hulot, G., 1997. Stationary and nonstationary behaviour within the geomagnetic polarity time scale. *Geophys. Res. Lett.* 24, 1875–1878.
- Gillen, K.P., Evans, M.E., 1989. New geomagnetic paleosecular-variation results from the Old Crow Basin, Yukon Territory, and their use in stratigraphic correlation. *Can. J. Earth Sci.* 26, 2507–2511.
- Glatzmaier, G.A., Roberts, P.H., 1995. A three-dimensional self-consistent computer simulation of a geomagnetic field reversal. *Nature* 377, 203–209.
- Glatzmaier, G.A., Coe, R.S., Hongre, L., Roberts, P.H., 1999. The role of the Earth's mantle controlling the frequency of geomagnetic reversals. *Nature* 401, 885–890.
- Gradstein, F.M., Agterberg, F.P., Ogg, J.G., Hardenbol, J., van Veen, P., Thierry, J., Huang, Z., 1995. A Triassic, Jurassic and Cretaceous time scale. In: Berggren, W.A., Kent, D.V., Aubry, M.-P., Hardenbol, J. (Eds.), *Geochronology Time Scales and Global Stratigraphic Correlation*. SEPM Special Publications, No. 54, pp. 95–126.
- Greff-Lefftz, M., Legros, H., 1999. Core rotational dynamics and geological events. *Science* 286, 1707–1709.
- Gubbins, D., 1987. Mechanisms for geomagnetic polarity reversals. *Nature* 326, 167–169.
- Gubbins, D., 1999. The distinction between geomagnetic excursions and reversals. *Geophys. J. Int.* 137, F1–F3.
- Hedlin, M.A., Evans, M.E., 1987. A palaeomagnetic study of some Pleistocene sediments in northern Canada and its bearings on the secular variation of the geomagnetic field. *Geophys. J. R. Astron. Soc.* 90, 693–703.
- Heslop, D., Dekkers, M.J., 2002. Spectral analysis of unevenly spaced climatic time series using CLEAN: signal recovery and derivation of significance levels using a Monte Carlo simulation. *Phys. Earth Planet. Inter.* 130, 103–116.
- Hollerbach, R., Jones, C.A., 1993. Influence of the Earth's inner core on geomagnetic fluctuations and reversals. *Nature* 365, 541–543.
- Johnson, C.L., Constable, C.G., 1997. The time-averaged geomagnetic field: global and regional biases for 0–5 Ma. *Geophys. J. Int.* 131, 643–666.
- Kruiver, P.P., Dekkers, M.J., Langereis, C.G., 2000. Secular variation in Permian red beds from Dôme de Barrot, SE France. *Earth Planet. Sci. Lett.* 179, 205–217.
- Kuang, W., Bloxham, J., 1997. An Earth-like numerical dynamo model. *Nature* 389, 371–374.
- Larson, R.L., Olson, P., 1991. Mantle plumes control magnetic reversal frequency. *Earth Planet. Sci. Lett.* 107, 437–447.
- Laskar, J., 1990. The chaotic motion of the solar system—a numerical estimate of the size of the chaotic zones. *Icarus* 88, 266–291.
- Lean, C.B., Latham, A.G., Shaw, J., 1995. Palaeosecular variation from a Vancouver Island stalagmite and comparison with contemporary North American records. *J. Geomagn. Geoelectr.* 47, 71–87.
- Loper, D.E., 1992. On the correlation between mantle plume flux and the frequency of reversals of the geomagnetic field. *Geophys. Res. Lett.* 19, 25–28.
- Loper, D.E., McCartney, K., 1986. Mantle plumes and the periodicity of magnetic field reversals. *Geophys. Res. Lett.* 13, 1525–1528.
- Lund, S.P., Banerjee, S.K., 1985a. Late Quaternary paleomagnetic field secular variation from two Minnesota lakes. *J. Geophys. Res.* 90, 803–825.
- Lund, S.P., Banerjee, S.K., 1985b. The paleomagnetic record of Late Quaternary secular variation from Anderson Pond, Tennessee. *Earth Planet. Sci. Lett.* 72, 219–237.
- Lund, S.P., Liddicoat, J.C., Lajoie, K.R., Henyey, T.L., Robinson, S.W., 1988. Paleomagnetic evidence for long-term (10^4 years) memory and periodic behavior in the Earth's core dynamo process. *Geophys. Res. Lett.* 15, 1101–1104.
- McElhinny, M.W., Lock, J., 1996. IAGA paleomagnetic databases with ACCESS. *Survey Geophys.* 17, 575–591.
- McElhinny, M.W., McFadden, P.L., 1997. Palaeosecular variation over the past 5 Myr based on a new generalized database. *Geophys. J. Int.* 131, 240–252.
- McElhinny, M.W., McFadden, P.L., Merrill, R.T., 1996. The time-averaged paleomagnetic field 0–5 Ma. *J. Geophys. Res.* 101, 25007–25027.
- McFadden, P.L., McElhinny, M.W., 1984. A physical model for palaeosecular variation. *Geophys. J. R. Astron. Soc.* 78, 809–830.
- McFadden, P.L., Merrill, R.T., 1995. Fundamental transitions in the geodynamo as suggested by paleomagnetic data. *Phys. Earth Planet. Inter.* 91, 253–260.
- McFadden, P.L., Merrill, R.T., 1997. Asymmetry in the reversal rate before and after the Cretaceous Normal Polarity Superchron. *Earth Planet. Sci. Lett.* 149, 43–47.
- McFadden, P.L., Merrill, R.T., McElhinny, M.W., Lee, S., 1991. Reversals of the Earth's magnetic field and temporal variations of the dynamo families. *J. Geophys. Res.* 96, 3923–3933.
- Nurgaliev, D.K., Borisov, A.S., Heller, F., Burov, B.V., Jasonov, P.G., Khasanov, D.I., Ibragimov, S.Z., 1996. Geomagnetic secular variation through the last 3500 years as recorded by Lake Aslikul sediments from eastern Europe (Russia). *Geophys. Res. Lett.* 23, 375–378.
- Olson, P., Hagee, V.L., 1990. Geomagnetic polarity reversals, transition field structure and convection in the outer core. *J. Geophys. Res.* 95, 4609–4620.
- Opdyke, N.D., 1995. Magnetostratigraphy of Permian-Carboniferous time. In: Berggren, W.A., Kent, D.V., Aubry, M.-P.,

- Hardenbol, J. (Eds.), *Geochronology Time Scales and Global Stratigraphic Correlation*. SEPM Special Publications, No. 54, pp. 41–47.
- Peck, J.A., King, J.W., Colman, S.M., Kravchinsky, V.A., 1996. An 84-kyr paleomagnetic record from the sediments of Lake Baikal, Siberia. *J. Geophys. Res.* 101, 11365–11385.
- Peng, L., King, J.W., 1992. A Late Quaternary geomagnetic secular variation record from Lake Waiiau, Hawaii, and the question of the Pacific nondipole low. *J. Geophys. Res.* 97, 4407–4424.
- Roberts, D.H., Lehár, J., Dreher, J.W., 1987. Time series analysis with clean. I. Derivation of a spectrum. *Astron. J.* 93, 968–989.
- Rochette, P., Ben Atig, F., Collombat, H., Vandamme, D., Vlag, P., 1997. Low secular variation at the equator: a paleomagnetic pilgrimage from Galapagos to Esterel with Allan Cox and Hans Zijderveld. *Geologie en Mijnbouw* 76, 9–19.
- Sheridan, R.E., 1986. Pulsation tectonics as the control of North Atlantic palaeoceanography. In: Summerhayes, C.P., Shackleton, N.J. (Eds.), *North Atlantic Palaeoceanography*. Geological Society of Special Publications, No. 21, pp. 255–275.
- Thouveny, N., Crear, K.M., Blunk, I., 1990. Extension of the Lac du Bouchet palaeomagnetic record over the last 120,000 years. *Earth Planet. Sci. Lett.* 97, 140–161.
- Turner, G.M., 1987. A 5000 years geomagnetic palaeosecular variation record from western Canada. *Geophys. J. R. Astron. Soc.* 91, 103–121.
- Turner, G.M., Thompson, R., 1979. Behaviour of the Earth's magnetic field as recorded in the sediment of Loch Lomond. *Earth Planet. Sci. Lett.* 42, 412–426.
- Turner, G.M., Thompson, R., 1981. Lake sediment record of the geomagnetic secular variation in Britain during Holocene times. *Geophys. J. R. Astron. Soc.* 65, 703–725.
- Turner, G.M., Thompson, R., 1982. Detransformation of the British geomagnetic secular variation record for Holocene times. *Geophys. J. R. Astron. Soc.* 70, 789–792.
- Turner, G.M., Evans, M.E., Hussin, I.B., 1982. A geomagnetic secular variation study (31 000–19 500 bp) in western Canada. *Geophys. J. R. Astron. Soc.* 71, 159–171.
- Vandamme, D., 1994. A new method to determine paleosecular variation. *Phys. Earth Planet. Int.* 85, 131–142.
- van den Ende, C., 1977. *Palaeomagnetism of Permian Red Beds of the Dôme de Barrot (S. France)*. Ph.D. Thesis. Rijksuniversiteit Utrecht, Utrecht, 171 pp.
- Verosub, K.L., Mehringer, P.J., Waterstraat, P., 1986. Holocene secular variation in western North America: paleomagnetic record from Fish Lake, Harney County, Oregon. *J. Geophys. Res.* 91, 3609–3623.
- Visscher, H., Huddleston Slater-Offerhaus, M.G., Wong, T.E., 1974. Palynological assemblages from Saxonian deposits of the Saar-Nahe Basin (Germany) and the Dôme de Barrot (France)—an approach to chronostratigraphy. *Rev. Palaeobot. Palynol.* 17, 39–56.
- Wardlaw, B.R., 2000. Notes from the SPS Chair. *Permophiles* 36, 1–2.
- Yugan, J., Wardlaw, B.R., Glenister, B.F., Kotlyar, G.V., 1997. Permian chronostratigraphic subdivisions. *Episodes* 20, 10–15.